

# Detecting Good Quality Frames in Videos Captured by a Wearable Camera for Blind Navigation

Long Tian, Yingli Tian

Dept. of Electrical Engineering

The City College, City University of New York  
New York, USA  
[{ltian00, ytian}@ccny.cuny.edu](mailto:{ltian00, ytian}@ccny.cuny.edu)

Chucai Yi

Dept. of Computer Science

The Graduate Center, City University of New York  
New York, USA  
[CYi@gc.cuny.edu](mailto:CYi@gc.cuny.edu)

**Abstract**—Recent technology developments in computer vision, digital cameras, and portable computers make it possible to assist blind individuals by developing camera-based object recognition products. However, motion blur caused by a moving camera limits the real-world application of wayfinding for blind users. In this paper, we propose a new method to detect good quality frames from videos captured by cameras, which are taken by blind users. In our proposed method, both gradient and intensity statistics are extracted from video frames. Then a support vector machine (SVM) based classifier is applied to identify the frames with good quality (Unblurred) from those blurred frames. The Unblurred frames will be further processed to extract essential information for blind wayfinding and navigation such as signage recognition and text extraction. Experimental results demonstrate that our proposed method is able to robustly handle video motions in both indoor and outdoor environments.

**Keywords**—*Blind, Navigation, Wayfinding, Motion blur, Video quality.*

## I. INTRODUCTION

According to the World Health Organization investigation in 2010 [1], 4.24% of the world's total population is suffering visual impaired and 0.58% persons are blind. This number is likely to increase rapidly as the baby boomer generation ages. Accessing unfamiliar environments is a very challenging task for blind people and can present life threatening situations. The ability of people who are blind or have significant visual impairments to access, understand, and explore unfamiliar environments will improve their inclusion and integration into society. It will also enhance employment opportunities, foster independent living, and produce economic and social self-sufficiency. To help the visual impaired people, many different kinds of assistant systems are developed over the last fifty years including video magnification [2], reading machines [3], text-to-speech (TTS) and screen readers [4], sonic travel guide[5, 6]. There are many camera-based aids such as signage recognition [12], text extraction [11, 14], bill recognition [13], navigation [7, 8, 9, 10, 15, 16] etc. These technologies invent to increase quality of life for millions of individuals with vision loss by allowing independent access unfamiliar environments.

Recent technology developments in computer vision, digital cameras, and portable computers make it possible to assist blind individuals by developing camera-based object recognition products. Our group has developed a number of new methods for assistive technologies to help blind people [9,

11-13]. In particular, our proposed solution of scene text extraction from natural scene images significantly outperforms most existing methods. However, these methods mainly focus on static images or videos without motion blur, which limit the real applications to assist blind people. Motion blur, as one of the most commonly encountered problems with mobile camera-based systems caused by the irregular motions of blind users who are wearing the camera, can significantly decrease the performance for blind wayfinding and navigation.

Unlike people with normal vision who can accurately aim on the target into the camera view, people who are blind normally cannot aim the camera accurately to the target therefore will not be able to keep the camera stable while taking images. The motion will cause blurry of images and will make camera-based wayfinding and navigation system fail. To our knowledge, no existing wayfinding assistant can handle motion blur and recognize text and signage to identify targeted destinations in challenging environments. Figure 1 shows that our camera-based blind-assist prototype system for wayfinding and navigation which includes a wearable camera mounted on a sun glasses, a mini computer for data processing, a microphone for speech command, and a Bluetooth ear piece for providing feedback to the blind user. Some example images captured by a wearable camera, as shown in Figure 2, are blurred due to the camera motion.

In this paper, we propose a new method to detect good quality frames from blurred frames in videos captured by wearable cameras while the blind users are moving. Our proposed method is robust to handle video motions in both indoor and outdoor environments by combining gradient features and statistical features of frequency, entropy, etc. Then a support vector machine (SVM) based learning model is applied to identify the frames with good quality (unblurred) from those blurred frames. The unblurred frames will be further processed to extract essential information such as sign and text from surrounding environment..

This paper is organized as follows. In Section II, we describe the related work of image quality assessment. Section III provides an overview of the proposed method. Section IV explains the features and classification to identify blurred and unblurred frames from video sequences. The experimental results and evaluation are presented in Section V. Section VI demonstrates some results of the text detection from blurred and unblurred images. Section VII concludes the paper and discusses our future work.



Fig. 1. Testing our prototype system with a wearable camera for blind navigation.



Fig. 2. Low-quality images captured by a wearable camera which are blurred. It will be difficult to extract necessary information from these blurred images for navigation such as text and signage etc.

## II. RELATED WORK OF IMAGE QUALITY ASSESSMENT

There are three types of methods for the image quality assessment including full-reference based [19, 33], reduced-reference based [20] and no-reference based methods [21-24, 32, 34, 35, 37]. For the full-reference based algorithms, the original sharp image with good quality is used as the reference image to compare with the test images for the quality difference. In reduced-reference methods, instead of using the whole image, part of information in original image is used as reference information. Recently, researchers have developed no-reference algorithms without using any knowledge of the original high quality images. For our task, detecting blur frames in video, there is no original high quality frames available, therefore, our method belongs to no-reference method.

The most popular features for non-reference image quality assessment are the edge features [21, 22]. Normally, the edge width of blurred images is larger than the edge width from clear images with good quality. In addition to edge width, edge gradient and slopes are also used for image quality assessment [32]. Furthermore, frequent space, transform-based and hybrid metrics are investigated by some researchers [29-31].

Considering the human visual perception system for edge changes, Ferzli and Karam proposed an algorithm based on cumulative probability of blur detection (CPBD) by introducing a measurement called "just noticeable blur (JNB)" to indicate the tolerance of human visual system for edge width changes [21]. Mittal et al. [37] demonstrated that the statistics of all pixels illumination in an image can be applied for the image quality assessment [37]. Ruderman proposed mean subtracted contrast normalized (MSCN) coefficients for image

representation which is the other form of normalized luminance coefficients [25]. The image quality distortion will affect the MSCN coefficients distribution function, which will be quantized with the parameter change in a distribution function. This blind and referenceless image spatial quality evaluator (BRISQUE) is enough efficient to be applied to the real-time image quality assessment.

Although many methods have been developed, the accuracy of the existing methods is not high enough for our blur detection task in blind navigation application. Therefore, in this paper, we propose a new method for blurred and unblurred image identification by combining the edge, luminance and statistics information.

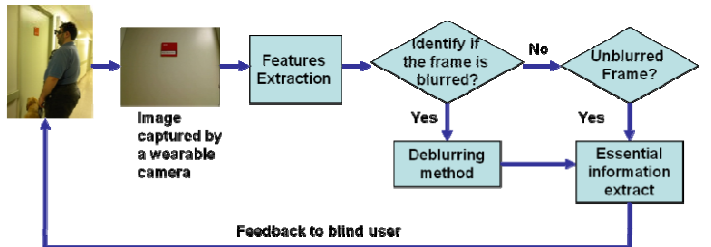


Fig. 3. The flowchart of the proposed method for detecting good quality frames from blurred frames from videos captured by a wearable camera.

## III. OVERVIEW OF THE PROPOSED METHOD

The flowchart of our proposed method to detect good quality images from blurred frames in videos captured by a wearable camera is shown in Figure 3. We observe that the edges in blurred frames are wider than the edges from frames with good quality. Therefore, we employ the edge information as the main features to classify blurred and unblurred frames. For each frame, edge and statistic features are first extracted. Then a SVM-based classifier is employed to detect if the frame is blurred or not. If the frame is unblurred, the essential information in this frame is extracted and provided to blind users as feedback in speech. If all the frames in a short period time are blurred, a deblurring processing will be applied and the essential information will then be extracted from the deblurred image. Due to the space limitation, the deblurring method is not included in this paper.

## IV. BLURRED AND UNBLURRED IMAGE CLASSIFICATION

### A. Features for Blurred and Unblurred Image Classification

In order to classify unblurred and blurred images from videos captured by wearable cameras, we extract 4 types of features based on both edge and luminance information: (1) average edge width, (2) average luminance, (3) cumulative edge blur probability, and (4) MSCN distribution [37]. More details are described as following:

- **Average edge width:** As shown in the 2nd row of Figure 4, we observe that even the edges in blurred frames are much less than the unblurred frames, the width of edges in blurred frames are normally wider than that from frames with good quality. Therefore, edge width will be a good feature to measure the image quality. To calculate the average edge width, we first apply a Sobel edge detector to the image. Then, in the perpendicular direction of the edge

gradient angle, the edge width for each edge pixel is calculated by the distance between the start and end positions of the edge pixel, which are defined as the local extreme locations closest to the edge pixel [36]. At last, the average value of width of each edge pixel for the whole frame is calculated as the average edge width feature. As shown in the 3rd row of Figure 4, the map of edge width distribution demonstrates that the maximum edge width for the blurred image (left) is larger than 30 pixels, while the edge width for the unblurred image (right) for most pixels is smaller than 15 pixels. Therefore, the average edge width is a good feature to classify unblurred and blurred images.

- **Average luminance:** For blind wayfinding and navigation, the indoor videos generally are more sensitive to the motion blur than outdoor videos since the distance between the camera and objects in outdoor environments is normally larger than that in indoor environments. Another difference between indoor and outdoor environments is the luminance difference. Generally, the average luminance of video frames for an outdoor environment in day time is larger than an indoor environment. Therefore, the feature of average luminance is applied in our method to model the environment luminance situation.
- **Cumulative edge blur probability:** In addition to the edge and luminance information, the human blur perception has different sensitivity with varying contrast values. At first, the image will be uniformly divided into patches (the patch size is selected as 64\*64 in our implementation). If the patch contains enough number of edges pixel (0.2% of the total pixels in patch), we will label it as ‘edge patch’ and process it in later steps. Then, the probability of blur detection for each edge in an “edge patch” is calculated. At last the edge values of the whole image are pooled by the calculating the cumulative edges blur probability of image for blur detection. More details of the calculation for the cumulative edge blur probability can be found in [22].
- **The mean subtracted contrast normalized (MSCN) luminance distribution:** Ruderman’s work demonstrates that the distribution of MSCN coefficients for an image is close to a generalized Gaussian distribution model (GGD) [25]. For the diagonal neighbor pixels in MSCN luminance image, the distribution follows an asymmetric generalized Gaussian distribution (AGGD) model [37]. In the last row of Figure 4, examples of MSCN distributions for blurred and unblurred frames are displayed. We observe that the distributions of MSCN are very different for blurred and unblurred frames. As shown in the following section, the parameters of GGD and AGGD are employed to measure the blur level of images.

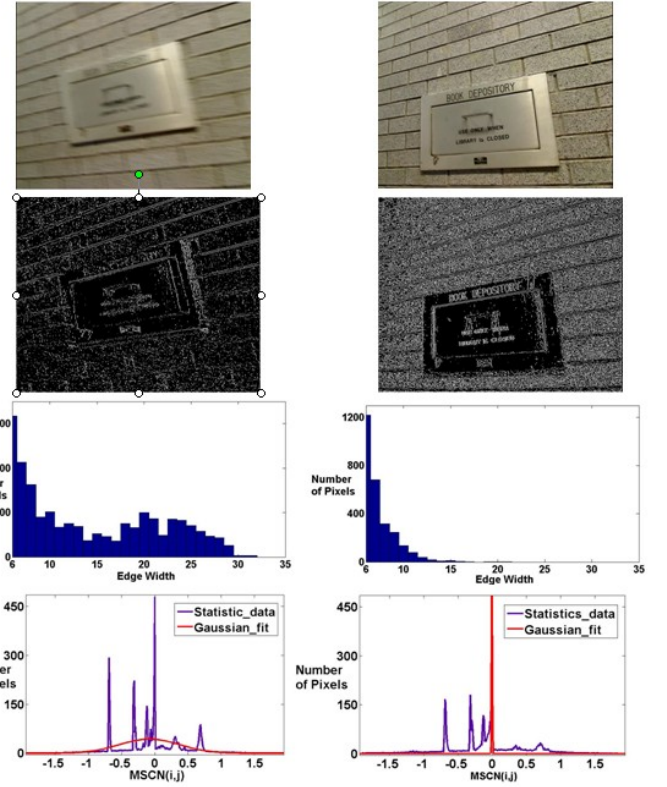


Fig. 4. The edge width and MSCN distribution for the blurred (left column) and unblurred (right column) frames. First row: original images; Second row: edge images; third row: edge width distributions; last row: MSCN distributions.

### B. Computation of MSCN Distributions

The mean subtracted contrast normalized (MSCN) luminance for pixel  $(i, j)$  is  $\hat{I}(i, j)$  which can be defined as [37]:

$$\hat{I}(i, j) = \frac{I(i, j) - \mu(i, j)}{\sigma(i, j) + C}, \quad (1)$$

where  $\mu(i, j)$  is the local mean of position  $(i, j)$ , calculated from a  $K*L$  neighborhood around it (we set  $K$  and  $L$  as 3 in the experiments), and  $\sigma(i, j)$  denotes the standard deviation of  $I(i, j)$  within the block.

$$\mu(i, j) = \sum_{k=-K}^K \sum_{l=-L}^L \omega_{k,l} I_{k,l}(i, j) \quad (2)$$

$$\sigma(i, j) = \sqrt{\sum_{k=-K}^K \sum_{l=-L}^L \omega_{k,l} (I_{k,l}(i, j) - \mu(i, j))^2}. \quad (3)$$

where  $\omega_{k,l}$  is a 2D circularly-symmetric Gaussian weighting function sampled out to 3 standard deviations and rescaled to unit volume.

The GGD model with zero mean is:

$$f(x; \alpha_1; \sigma^2) = \frac{\alpha_1}{\beta \Gamma\left(\frac{1}{\alpha_1}\right)} \exp\left(-\left(\frac{|x|}{\beta}\right)^{\alpha_1}\right), \quad (4)$$

where  $\beta = \sigma \sqrt{\frac{\Gamma\left(\frac{1}{\alpha_1}\right)}{\Gamma\left(\frac{3}{\alpha_1}\right)}}$  and  $\Gamma(\ )$  is the gamma function:

$$\Gamma(a) = \int_0^{\infty} t^{a-1} e^{-t} dt \quad a > 0, t \text{ is real number.}$$

For neighboring MSCN coefficients, the AGGD model is :

$$f(x; \alpha_2; \sigma_l^2; \sigma_r^2) = \begin{cases} \frac{\alpha_2}{(\beta_l + \beta_r)\Gamma\left(\frac{1}{\alpha_2}\right)} \exp\left(-\left(\frac{-x}{\beta_l}\right)^{\alpha_2}\right) & x < 0 \\ \frac{\alpha_2}{(\beta_l + \beta_r)\Gamma\left(\frac{1}{\alpha_2}\right)} \exp\left(-\left(\frac{-x}{\beta_r}\right)^{\alpha_2}\right) & x \geq 0 \end{cases} \quad (5)$$

$$\text{where } \beta_l = \sigma_l \sqrt{\frac{\Gamma\left(\frac{1}{\alpha_2}\right)}{\Gamma\left(\frac{3}{\alpha_2}\right)}} \text{ and } \beta_r = \sigma_r \sqrt{\frac{\Gamma\left(\frac{1}{\alpha_2}\right)}{\Gamma\left(\frac{3}{\alpha_2}\right)}}.$$

The parameter  $\sigma$  indicates the GGD variance and  $\alpha_1$  control the GGD shape. We employ  $(\sigma, \alpha_1)$  and  $(\sigma_l, \sigma_r, \alpha_2)$  as our features, where  $\sigma_l$  indicates the left side AGGD variance,  $\sigma_r$  respects the right side AGGD variance and  $\alpha_2$  control the AGGD shape.

### C. Feature Normalization

To input the features into SVM learning model to identify the frame is blurred or unblurred, the features are normalized into the range [0, 1]. In our experiments, each feature has a different range. For example, the average edge width value is from 5 to 30, and the average luminance is around 50. After this normalization, all the features are ready for detecting blurred images.

### D. SVM-based Blurred and Unblurred Image Classification

For SVM-based blurred and unblurred image classification, training dataset with the features and labels  $(x_i, y_i)$  where  $x_i$  is the collected features and  $y_i \in \{1, -1\}$  is the label of categories. In this paper, the C-SVM classification is applied and it should complete the solution for the optimization problem:

$$\min_{w, b, \xi} \frac{1}{2} w^T w + C \sum_{i=1}^l \xi_i \quad (6)$$

$$\text{subject to } y_i (w^T \phi(x_i) + b) \geq 1 - \xi_i \quad \xi_i \geq 0 \quad (7)$$

where  $\xi_i$  is non-negative slack variables, which measure the degree of misclassification of the data  $x_i$ ,  $w$  is the weight vector,  $b$  is the bias and  $C$  is per-chosen parameter which will affect the accuracy performance of SVM.

The kernel function is:  $K(x_i, x_j) = \phi(x_i)^T \phi(x_j)$ , where  $\phi$  is the function to map training vectors  $x_i$  into a high dimensional space. The radial basis function (RBF) is applied as kernel function because it was found to be the most effective function:

$$K(x_i, x_j) = \exp(-\gamma \|x_i - x_j\|^2) \quad (8)$$

The SVM classifier needs RBF kernel function with two parameters  $(C, \gamma)$ , which need to be adjusted for the small number of support vectors that will reduce the calculating time.



Fig. 5 The blurred (left column in a and b) and unblurred (right column in a and b) example images in our dataset.

## V. EXPERIMENTS

### A. Database

To evaluate the proposed method as shown in Figure 1, we develop a blind assistant prototype system including a Logitech HD webcam mounted on a pair of sunglasses and a mini laptop for data analysis. The videos are captured from both outdoor and indoor environments while the user is moving around. The image resolution is 1240\*1024 pixels. In total, we capture 17 videos including 7 outdoor videos and 10 indoor videos. The blurred and unblurred frames are manually labeled for the algorithm evaluation based on human visual perception. The frames we selected from these videos for training and testing mainly consist of the meaningful information, such as entrances, characters, text and signage information which could be valuable for blind person. Table I shows the total number of frames selected from all the captured videos as blurred and unblurred group. The total number of frames for our method is

948, including 512 blurred frames and 436 unblurred frames. For the training group, 715 frames are selected, and the testing group contains 233 frames. Some example images are shown in Figure 5.

TABLE I. NUMBER OF FRAMES OF BLURRED AND UNBLURRED FOR TRAINING AND TESTING

	Training Group		Testing Group	
	Blurred	Unblurred	Blurred	Unblurred
Indoor	224	193	61	42
Outdoor	147	151	80	50

### B. Results and Analysis

As mentioned in Section IV-A, 4 types of features are extracted from each frame, which are average edge width, average luminance, cumulative edge blur probability, and MSCN luminance distributions. The CPBD [21] and BRISQUE [25] algorithms are adopted in our experiments for performance comparisons. CPBD method has the best performance for the non-SVM frame blur detection in videos and BRISQUE could perform blur detection with SVM in real time.

TABLE II. ACCURACY OF OUR METHOD AND OTHER METHODS

	CPBD [21]	BRISQUE [25]	Our method
Blurred	78.7%	52.5%	78.7%
Unblurred	81.5%	82.6%	92.4%
Total	79.8%	64.4%	84.1%

The performance comparison of our method and the state-of-the-art methods is displayed in Table II. The model of SVM we applied is the C-SVM classification which satisfies Equations (6) and (7), the parameters  $C$  and  $\gamma$  are set as 2.1 and 1/8 respectively. Our method outperforms both CPBD and BRISQUE algorithms. Comparing to the CPBD method, the average accuracy of our method is about 4% higher accuracy, and the accuracy for the unblurred detection (good quality) frames is 11% higher while the accuracy in blurred frame detection is almost the same. The reason for this varying result might come from the different sensitive of human visual system for blurred and unblurred frames. Normally, human visual system is more sensitive to the varying of blurred level, but it is hard to tell the different of two unblurred frames. In this case, it is easy to detection unblurred frames based on the human visual system pre-labeled dataset. On the other hand, selecting good quality (the unblurred) frames is the main research focus for our application to directly extract text information directly from them.

We further evaluate our method for indoor and outdoor environments respectively. The evaluation results are shown in Figure 6. Comparing to other methods, our method achieves the best performance in both the indoor environment (around 10% higher than CPBD and 30% higher than BRISQUE), and in the outdoor environment. Our method achieves almost the same accuracy as CPBD method (around 85%) and about 14% higher accuracy than BRISQUE. For the indoor condition, the background luminance is relatively low, which could affect the contrast just notable blur judgment in CPBD algorithm. Our

method combines the luminance features in our system which can help to overcome the limitations of CPBD method.

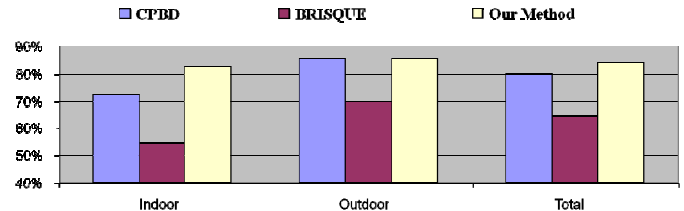


Fig.6 The blurred detection accuracy in outdoor and indoor environment.

### VI. EXTRACT TEXT INFORMATION

Signage with text is the most reliable labels for destination recognition in the application of blind wayfinding and navigation. Text is generally surrounded by all kinds of background outliers. To help blind users find their destinations through surrounding text information in an unfamiliar environment, we have proposed several text detection algorithms to find the text from scene images [11, 28]. Although the algorithms are able to handle text strings in different fonts, sizes, and colors, , they cannot obtain good performance in blurred images, so the quality of captured images limits the application of computer vision-based blind assistance.

The method described in this paper can be used as a pre-processing component for assistive blind navigation system. To demonstrate the benefits of our proposed method in image-based information retrieval, we apply scene text detection to the low-quality blurred images and the good quality images selected by the proposed method. Some results are shown in Figure 7. The localized text regions are marked by blue rectangle boxes, which will be further processed for text recognition. We observe that more true positive text regions are successfully detected in the good quality images.



Fig. 7 Exsample results of text information extraction from blurred images (top row) and unblurred images (bottom row). It shows that the scene text extraction results are more reliable on unblurred images.

### VII. CONCLUSION

In this paper, we have proposed a new method to select good quality frames in videos, which could improve the navigation and wayfinding system for blind users. To improve the accuracy and robustness, we extract features by combining edge information, average luminance, and luminance distributions. The proposed method has been evaluated by the

self-collected database. The evaluation results demonstrate that our method outperforms the state-of-the-art methods. Our future work will focus on improving the accuracy, robustness, and efficiency of the proposed method.

#### ACKNOWLEDGMENT

This work was supported in part by NSF grants EFRI-1137172, IIP-1343402, and FHWA grant DTFH61-12-H-00002.

#### REFERENCES

- [1] Factsheet of World Health Organization, Visual impairment and blindness, <https://apps.who.int/inf-fs/en/fact230.htm>
- [2] S. M. Genensky, P. Baran, H. Moshin, and H. Steingold, "A closed circuit TV system for the visually handicapped," 1968.
- [3] R. Kurzweil, "The Kurzweil reading machine: A technical overview," *Science, Technology and the Handicapped*, pp. 3–11, 1976.
- [4] A. Arditì and A. Gillman, "Computing for the blind user," *Byte*, vol. 11, no. 3, pp. 199–211, 1986.
- [5] L. Kay, "A sonar aid to enhance spatial perception of the blind: Engineering design and evaluation," *Radio and Electronic Engineer*, vol. 44, no. 11, pp. 605–627, 1974.
- [6] A. D. Heyes, "The Sonic Pathfinder: A New Electronic Travel Aid," *Journal of Visual Impairment and Blindness*, vol. 78, no. 5, pp. 200–02, 1984.
- [7] P. Meijer, "Seeing with sound -- the vOICe." [Online]. Available: <http://www.seeingwithsound.com>.
- [8] "VizWiz - Take a Picture, Speak a Question, and Get an Answer." [Online]. Available: <http://vizwiz.org/>. [Accessed: 10-Mar-2013].
- [9] Y. Tian, X. Yang, C. Yi, and A. Arditì, "Toward a Computer Vision-based Wayfinding Aid for Blind Persons to Access Unfamiliar Indoor Environments," *Machine Vision and Applications*, Issue 24, No. 3, April 2013, pp. 521-535..
- [10] Y. Danilov and M. Tyler, "Brainport: an alternative input to the brain," *Journal of integrative neuroscience*, vol. 4, no. 4, pp. 537–550, 2005.
- [11] C. Yi and Y. Tian, "Assistive text reading from complex background for blind persons," *ICDAE Workshop on Camera-based Document Analysis and Recognition (CBDAR)*, Springer LNCS-7139, 15-28, 2011.
- [12] S. Wang, C. Yi, and Y. Tian, "Signage Detection and Recognition for Blind Persons to Access Unfamiliar Environments," *Journal of Computer Vision and Image Processing*, Vol. 2, No. 2, 2012.
- [13] F. Hasanuzzaman, X. Yang, and Y. Tian, Robust and Effective Component-based Banknote Recognition for the Blind, *IEEE Transactions on Systems, Man, and Cybernetics--Part C: Applications and Reviews*, Jan. 2012.
- [14] H. Shen and J. Coughlan, "Grouping using factor graphs: an approach for finding text with a camera phone," *Graph-Based Representations in Pattern Recognition*, pp. 394–403, 2007.
- [15] V. Ivanchenko, J. Coughlan, and H. Shen, "Crosswatch: A camera phone system for orienting visually impaired pedestrians at traffic intersections," *Computers Helping People with Special Needs*, pp. 1122–1128, 2008.
- [16] R. Manduchi, J. Coughlan, and V. Ivanchenko, "Search strategies of visually impaired persons using a camera phone wayfinding system," *Computers Helping People with Special Needs*, pp. 1135–1140, 2008.
- [17] R. Manduchi and J. Coughlan, "(Computer) vision without sight," *Communications of the ACM*, vol. 55, no. 1, pp. 96–104, 2012.
- [18] Y. Shen and L.Z. Ma, "Detecting and Removing the Motion Blurring from Video Clips," *I. J. Modern Education and Computer Science*, 1:17-23, 2010.
- [19] H. R. Sheikh, M. F. Sabir and C. Bovik, "A Statistical Evaluation of Recent Full Reference Image Quality Assessment Algorithms," *IEEE Transactions on Image Processing*, 15(11): 3411-3452, 2006.
- [20] Q. Li and Z. Wang, "Reduced-Reference Image Quality Assessment Using Divisive Normalization-Based Image Representation," *IEEE Journal of Selected Topics in Signal Processing*, 3(2): 202-211, 2009.
- [21] R. Ferzli and L. J. Karam, "A No-Reference Objective Image Sharpness Metric Based on the Notion of Just Noticeable Blur (JNB)," *IEEE Transactions on Image Processing*, 18(4): 717-728, 2009.
- [22] N. D. Narvekar and L. K. Karam, "A No-Reference Image Blur Metric Based on the Cumulative Probability of Blur Detection (CPBD)," *IEEE Transaction on Image Processing* 20(9): 2678-2683, 2011.
- [23] A. Ciancio, A. L. N. T. da Costa, E. A. B. da Silva, A. Said, R. Samadani and P. Obrador, "Objective No-Reference Image Blur Metric Based on Local Phase Coherence," *Electronics Letters* 45(23): 1162-1163, 2009.
- [24] S. Suresh, R. V. Babu and H. J. Kim, "NO-reference image quality assessment using modified extreme learning machine classifier," *Applied Soft Computing* 9: 541-552, 2009.
- [25] D. L. Ruderman, "The statistics of natural images," *Network: Computation in Neural Systems* 5:517-548, 1994.
- [26] X. Chen J. Yang, J. Zhang and A. Waibel, "Automatic detection and recognition of signs from natural scenes," *IEEE Transactions on Image Processing*, 13:87-99, 2004.
- [27] Y. C. Shiu and C. Huang, "Locating cylindrical objects from perspective projections," *Aerospace and Electronics Conference, 1991, NAECON 1991, Proceedings of the IEEE 1991 National*.
- [28] C. Yi and Y. Tian, "Text string detection from natural scenes by structure based partition and grouping," *IEEE Transactions on Image Processing*, 2011.
- [29] R. Hassen, Z. Wang and M. Salama, "No-reference image sharpness assessment based on local phase coherence measurement," *IEEE Int. Conf. Acoust., Speech and Signal Processing*, 2010.
- [30] P. Vu and D. Chandler, "A fast wavelet-based algorithm for global and local image sharpness estimation," *IEEE Signal Processing letter*, 19: 423-426, 2012.
- [31] M. Saad, A.C. Bovik and C. Charrier, "Blind image quality assessment: Anatural scen statistics approach in the DCT domain," *IEEE Trans. Image Process*. 21:3350-3364, 2011.
- [32] C. Feichtenhofer, H. Fassold and P. Schallauer, "A perceptual image sharpness metric based on local edge gradient analysis," *IEEE Signal Processing Letters*, 20: 379-382, 2013
- [33] Q. Chen, Y. Xu, C. Li, N. Liu, and X. Yang, "An image quality assessment metric based on quaternion wavelet transform," *IEEE IEEE International Conference on Multimedia & Expo*, 2013.
- [34] K. Gu, G. Zhai, X. Yang, W. Zhang and L. Liang, "No-Reference image quality assessment metric by combinig free energy theory and structural degradation model," *IEEE International Conference on Multimedia & Expo*, 2013.
- [35] W. Xue, L. Zhang and X. Mou, "Learning without human scores for blind image quality assessmetn," *IEEE Computer Vision and Pattern Recognition*, 2013.
- [36] P. Marziliano, F. Dufaux, S. Winkler and T. Ebrahimi, "A no-reference perceptual blur metric," *IEEE International Conference on Image Processing*, 3 57-60, 2002.
- [37] A. Mittal, A. K. Moorthy and A. C. Bovik, "No-Reference Image Quality Assessment in the Spatial Domain," *IEEE Transactions on Image Processing* 21(12) 4695-4708, 2012.